JOURNAL OF MATERIALS SCIENCE 30 (1995) 3407–3414

Influence of temperature and interelectrode distance on the negative differential resistance in metal–chalcogenide glassy semiconductors

M. DOMÍNGUEZ, E. MÁRQUEZ, P. VILLARES AND R. JIMÉNEZ-GARAY
Departamento de Estructura y Propiedades de los Materiales, Facultad de Ciencias, Universidad de Cádiz, Apdo. 40, 11510 Puerto Real (Cádiz), Spain

An investigation has been carried out, to elucidate some aspects of the current-controlled negative differential resistance (CCNDR) effect in bulk metal–chalcogenide glassy semiconductors. Because this phenomenon has been shown to be mainly of a thermal nature, a model, from the thermodynamic point of view, was developed, including some aspects related to the thermistors theory. The main conclusion from this model is the appearance of a current filament, which showed up when the material switched from the high electrical resistance to the low electrical resistance state, forming a crystalline filament between both electrodes. The variation of the CCNDR parameters with temperature and interelectrodic distance was studied, using both coplanar point electrodes and coplanar disc electrodes. The experimental results show a good agreement with the expected behaviour from the proposed thermal model (especially when natural convection was considered as the heat-exchanging process between the material and the ambient surrounding). In addition an algorithm was found to simulate the phenomenon computationally, using the experimentally determined physical parameters for the samples under study.

1. Introduction

There have been many studies on the electrical switching characteristics of chalcogenide glasses, since that reported by Ovshinsky [1], but the fields of technological applications of these materials, many of which have been developed through recent years, are not actually restricted to the switching effect, thus broadening the scope of study. Certainly, chalcogenide glassy semiconductors have proved to be of interest for optical [2, 3], electrochemical [4] and, of course, electrical applications [5]. Generally, chalcogenide glasses are characterized by high values of electrical resistivity, yielding serious limitations on applications as well as measurements. The addition of d-elements into these amorphous materials leads to very significant changes in their electrical conductivities [6]. In fact, copper has been used as a chemical modifier [7], showing a marked influence on the electrical conductivity.

One useful property widely shown by chalcogenide glassy semiconductors is the phenomenon called the current-controlled negative differential resistance (CCNDR) effect, typical of a thermistor or thermally sensitive resistor [8]. The CCNDR effect in chalcogenide semiconductors can be considered from different points of view, including both thermal and electronic effects [9, 10]. In the present work, an attempt has been made to confirm the fundamentally thermal nature of this effect, considering the influence on the CCNDR phenomenon of both ambient temperature [11] and interelectrode distance [12], by studying the electrical behaviour of the glassy alloy $Cu_{0.05}As_{0.50}Te_{0.45}$.

2. Experimental procedure

The bulk glassy semiconductor investigated, was obtained by the conventional melt–quench method [13], from elements of 99.999% purity, which were introduced into a quartz tube. This tube was subjected to several helium-filling and evacuation to $\approx 10^{-3}$ torr (1 torr = 133.322 Pa) operations, until it was definitively sealed at this final pressure. The ampoule thus obtained, was then introduced into a rotary furnace, heated to approximately 950 °C, and kept at this temperature for 4 h. Finally, the ampoule was quenched in water. The non-crystalline nature of the ingot obtained was confirmed by X-ray diffraction (XRD) and differential scanning calorimetric (DSC) analysis.

The fragments of the ingot, taken from the ampoule, were embedded in an epoxy-type resin and polished with 0.3 and 0.05 μm alumina powder, until mirror-like surfaces were obtained. In those experiments carried out at different ambient temperatures, with a fixed interelectrode distance of 2.3 mm, a coplanar point electrode configuration was used [14]. Temperature was regulated and controlled by a PID-type temperature controller (Omron E5K),

0022–2461

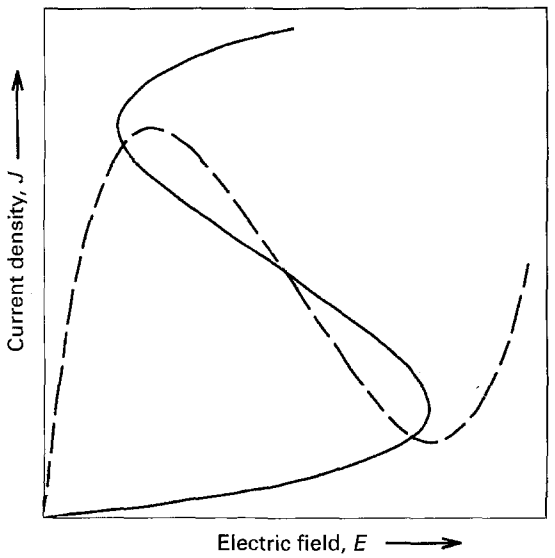

Figure 1 Typical current density–electric field characteristics showing the (—) CCNDR and (– – –) VCNDR phenomena.

which allows an accuracy better than $\pm 0.3\,^{\circ}C$. On the other hand, for those experiments involving different interelectrode distances, two copper discs adhered to the same surface of the sample by means of silver paste, were used as the electrode system. Finally, in both cases, the circuit used to find the steady-state current-voltage characteristics included a current source (Haake–Büchler model CVP2000).

3. A thermodynamical approach

The CCNDR effect is a phenomenon exhibited by those materials which have a negative coefficient of electrical resistance on temperature, i.e. the resistance decreases as temperature increases. In this case, when the current flowing through the glassy semiconductor is increased in sequence, allowing the sample to reach the thermal equilibrium at every step, the internal temperature of the sample also increases for each stage, decreasing the semiconductor electrical resistance as well. The voltage drop measured at this steady state, will be lower than that predicted by Ohm's law, and the differential resistance (dV/dI), will also be lowered step by step, if the current is increased. Finally, a maximum voltage is obtained (the so-called turnover voltage), when the differential resistance equals zero. Beyond this point, when increasing current values, the steady-state voltage falls to lower values, reaching the differential resistance a negative value. Typical steady-state current–voltage characteristics are shown in Fig. 1. Note the different behaviour of the CCNDR materials and voltage controlled negative differential resistance (VCNDR) materials.

A basic treatment of CCNDR has been provided through the framework of irreversible thermodynamics by Ridley [9], where, rather more than a discussion of the physical causes which originate this effect, the consequences of the appearance of this phenomenon, are considered. It should be emphasized that, as the CCNDR region is an electrically unstable zone, it can only be reached if the current is kept constant by means of the external circuit. When the CCNDR region is obtained in the steady state, the material, which was initially homogeneous from the electrical point of view, must split into two different regions, one of them being a high current filament running along the electrical field direction. If the current is not limited by the external circuit, the electrical switching of the chalcogenide glassy semiconductor occurred, in a thermal avalanche-type process [15, 16]. This is the reason why, in this work, a current source was used to obtain the experimental results, allowing the samples to achieve thermal equilibrium before readings were taken.

3.1. Basic thermodynamic equations

The CCNDR phenomenon has been analysed from the point of view of irreversible thermodynamics, applied to continuous systems [17]. Let us consider an electrically isotropic slab of material, of unit cross-sectional area and of unit length, in which potential and temperature gradients exist. Considering a constant volume system, the second law of thermodynamics (Gibbs equation) becomes

$$T\left(\frac{dS}{dt}\right) = \frac{dU}{dt} - \Sigma\mu_k\left(\frac{d\rho_k}{dt}\right) \tag{1}$$

where S is the entropy, U the total internal energy, μ_k the chemical potential for the kth component of the material (Gibbs specific function), and ρ_k, its density, i.e. $\rho_k = M_k/V$ (mass of the kth component per unit volume). When an electric field, $\boldsymbol{E}$, is established, the internal energy, U, referred to unit volume, is transformed into U^*, and μ_k into μ_k^*

$$U^* = U + \Sigma e_k \rho_k \Phi \tag{2}$$

$$\mu_k^* = \mu_k + e_k \Phi \tag{3}$$

where e_k is the specific electrical charge of the kth component, and Φ is the internal electrical potential.

The second basic equation is the energy balance expression

$$\frac{dU^*}{dt} = -\operatorname{div}\boldsymbol{J}_u + \Sigma e_k \rho_k \frac{d\Phi}{dt} \tag{4}$$

where $\boldsymbol{J}_u$ is the total energy flow, i.e. the sum of the heat flow, $\boldsymbol{J}_q$, and the electrical energy flow

$$\boldsymbol{J}_u = \boldsymbol{J}_q + \Sigma e_k \Phi \boldsymbol{J}_k \tag{5}$$

$\boldsymbol{J}_k$ being the flow of mass of the kth component.

The third equation is the mass conservation law, applied to each component, which can be written in the following way

$$\frac{d\rho_k}{dt} = -\operatorname{div}\boldsymbol{J}_k + \frac{\partial \rho_k}{\partial t} \tag{6}$$

Finally, the last equation is the net charge neutrality condition

$$\Sigma e_k \frac{\partial \rho_k}{\partial T} = 0 \tag{7}$$

Substituting Equations 2–7 into Gibb's equation, the change in the entropy with time can be obtained as follows

$$\frac{dS}{dt} = -\operatorname{div}\left(\frac{J_q - \Sigma\mu_k J_k}{T}\right) + \left[\frac{(J_q - \Sigma\mu_k J_k)\cdot X_q + E\cdot J + \Sigma\left(X_k\cdot J_k - \mu_k\frac{\partial\rho_k}{\partial t}\right)}{T}\right] \quad (8)$$

where E ($= -\operatorname{grad}\Phi$), is the electric field, J ($= \Sigma e_k J_k$), is the current flow, X_k ($= -\operatorname{grad}\mu_k$), is the diffusion "force" and, finally, X_q ($= T\operatorname{grad}(1/T)$) is the thermal "force". This expression can be rewritten as

$$\frac{dS}{dt} = -\operatorname{div} J_s + \dot{s} \quad (9)$$

which has the form of a balance equation. So, the entropy change is due to the divergence of an entropy flow and the entropy production (per unit volume and unit time), the latter being the sum of the products of the different energy flows and their corresponding "forces". Therefore, this entropy production rate is the result of the action of irreversible processes, such as the thermal and electrical conduction and the mass diffusion.

3.2. Conditions in the CCNDR region: the crystalline conductive filament

Here, the conditions for the material when a CCNDR region is reached, at the steady state [18] are studied. Considering Equation 9, this steady state can be defined as that at which all the mass and electrical charge flows, both perpendicular to the current direction, disappear. The entropy production will balance to the divergence of entropy flow, and so, dS/dt equals zero [9].

First, let us consider that the material is originally homogeneous from the standpoint of the electrical properties so that, as is shown in Fig. 2, for a certain electrical field, E_0, a current density, J_0, can be reached inside the CCNDR region. Secondly, it has been shown [9] that when the J–E characteristics of this material show a CCNDR region, it must split into two different zones: a narrow current filament, whose area is a fraction, b, of the whole material cross-sectional area between both electrodes, and the rest of the material, because this situation favours the existence of a CCNDR region. When this situation is established, according to Ridley [9], the entropy production rate is

$$\dot{s} = \dot{s}_1(1 - b) + \dot{s}_2 b \quad (10)$$

where subscripts 1 and 2 refer to the external and internal area of the filament, respectively. At steady-state conditions, the production of entropy is due mainly to the electrical energy:

$$\dot{s}_1 T = E_1 J_1 \quad (11)$$

$$\dot{s}_2 T = E_2 J_2 \quad (12)$$

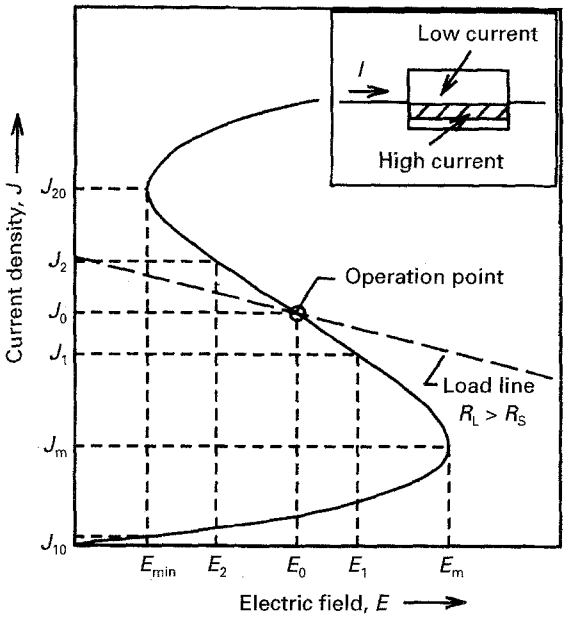

Figure 2 J–E characteristics for a CCNDR device, showing both the negative differential resistance and the second positive differential resistance regions. A schematic plot of the current filamentation is shown in the inset.

It is possible to express both the current density and the electrical field, in the filament and in the rest of the material, in terms of the initial values J_0, E_0

$$J_1 = J_0 + \Delta J_1 \quad (13)$$

$$J_2 = J_0 + \Delta J_2 \quad (14)$$

$$E_1 = E_0 + \Delta J_1\frac{dE}{dJ} \quad (15)$$

$$E_2 = E_0 + \Delta J_2\frac{dE}{dJ} \quad (16)$$

if the electric field increases linearly with current density. Assuming E_0 and J_0 are kept as average values, even after the current filamentation

$$J_1(1 - b) + J_2 b = J_0 \quad (17)$$

and also

$$\Delta J_1(1 - b) + \Delta J_2 b = 0 \quad (18)$$

Substituting Equations 11–18 into Equation 10, one can determine that the entropy production rate is given by

$$T\dot{s} = \left(\frac{1}{b} - 1\right)J_1^2\frac{dE}{dJ} \quad (19)$$

Considering that dE/dJ is the differential resistance, when this magnitude is negative, the entropy production rate will also be negative. So, the current filament formation at the CCNDR zone means a reduction of entropy production, i.e. it is a favourable condition from the view point of thermodynamics. On the other hand, from Equation 19, we can find that the entropy production rate is minimum whenever the heating by Joule effect, represented in Equation 19 by the term $J_1^2\,dE/dJ$, is minimum too.

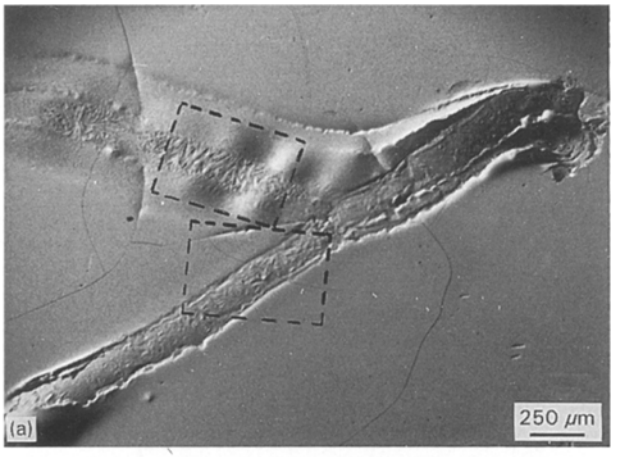

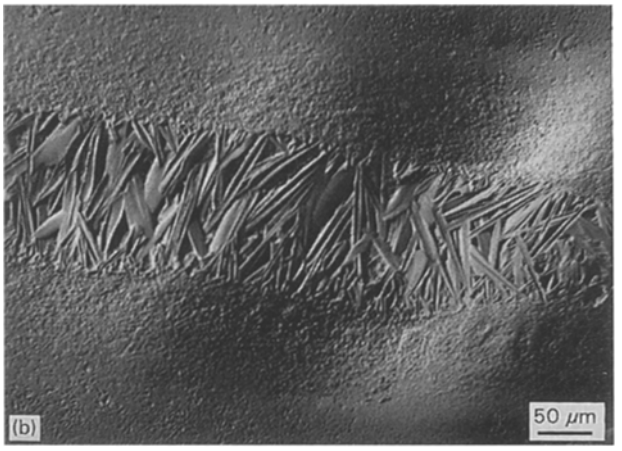

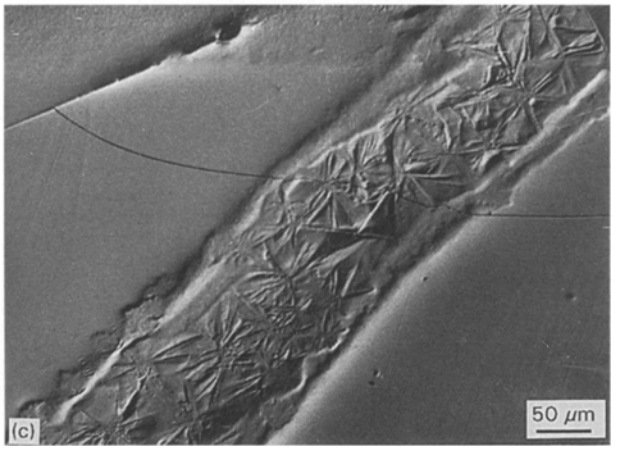

Figure 3 Scanning electron-micrographs showing (a) two memory filaments obtained in CCNDR experiments, (b) and (c) more detailed views of the zones marked in (a), showing the dendrite-like growth, characteristic of crystalline materials.

For each initial current density, J_0, many possible steady states can exist, all of them characterized by a filament of area b and an electric field E. The most favourable steady state will be that at which the electric field is a minimum, so that, if J_{10} and J_{20} are the values for the current density for minimum electrical field, E_{min} (see Fig. 2), for any other current level, such as J_0, for example, the filament area is given by the expression

$$b = \frac{J_0 - J_{10}}{J_{20} - J_0} \tag{20}$$

So, when the current is increased through the CCNDR region, the current filament area increases linearly, but when the differential resistance reaches its positive region, the filament is extended to the whole material area (so, $b = 1$).

For those materials showing the CCNDR phenomenon, the electrical stability inside this zone can only be reached in two ways: using a constant current source, or, with a constant voltage source, if the load resistor in the circuit, is greater than the material electrical resistance at the point of the CCNDR region considered, as shown in Fig. 2.

In chalcogenide glassy semiconductors, the CCNDR region has a well-established limit, as was shown elsewhere [11], and unfortunately, the second positive differential resistance cannot usually be reached. When a certain transitional current is reached, a sudden change in the electrical conductivity of the material occurred: the glassy semiconductor switches to a permanent low electrical resistance (or memory) state, appearing a crystalline conductive filament between the electrodes [11, 15]. This behaviour is typical of a negative differential resistance device with memory [19]. Fig. 3 shows some scanning electron micrographs of a conductive filament that appeared on a $Cu_{0.05}As_{0.50}Te_{0.45}$ sample, after the switching process had occurred in a CCNDR experiment, carried out with a double point contact electrode arrangement. The occurrence of this filament is additional evidence of current (and so, thermal) filamentation in the material, when the CCNDR effect appears. Several regions can be observed in these micrographs: first, the amorphous matrix, i.e. the zone of the material unchanged during electrical stimulation; secondly, between both electrodes, there is a region which melted during the electrical stimulation, and reamorphized after this stimulation was suppressed; finally, inside this melt–quenched zone, a narrow filament can be seen, showing dendrite-like growth, characteristic of crystalline materials. The crystalline nature of these filaments has been checked by X-ray diffraction, as reported in detail elsewhere for different chalcogenide glassy alloys [15]. Additionally, these scanning electron micrographs clearly show the influence between consecutively formed crystalline filaments [20].

4. A thermistor approach

4.1. Dependence of the turnover voltage on temperature

Thermistors are semiconductor devices, whose electrical resistance changes drastically with temperature [21]. It is worth mentioning that thermistors are used as temperature sensors, for thermal conductivity and radiation measurements, and also for control purposes [22]. Their current–voltage characteristics are those of the devices showing the CCNDR phenomenon: for a certain value I_m, it reaches a maximum voltage, V_m, which cannot be transcended, although the current is increased. Beyond this critical point, a negative differential resistance region appears.

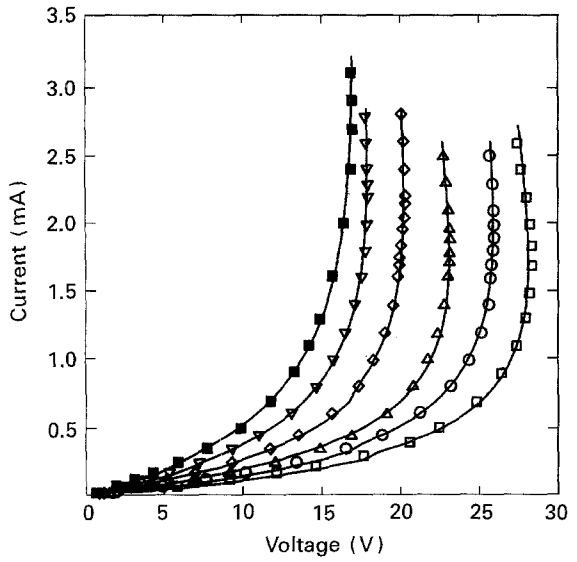

Figure 4 Steady-state current–voltage characteristics for glassy alloy $Cu_{0.05}As_{0.50}Te_{0.45}$, for different temperatures, with the CCNDR effect. (□) 24 °C, (○) 28 °C, (△) 34 °C, (◇) 40 °C, (▽) 46 °C, (■) 52 °C.

To obtain theoretically the current–voltage characteristics, consider the equations for electrical resistance as a function of temperature

$$R(T) = R_0 \exp\left(\frac{\Delta E}{k_B T}\right) \tag{21}$$

and

$$R(T) = \frac{V}{I} = R_a \exp\left[\left(\frac{1}{T} - \frac{1}{T_a}\right)\frac{\Delta E}{k_B}\right] \tag{22}$$

where R_0 is the pre-exponential factor of electrical resistance, R_a is the resistance at ambient temperature, T_a, ΔE is the activation energy for the thermally-activated mechanism of conductivity and k_B is the Boltzmann constant.

Now, we can consider the thermal balance equation in a simple form, assuming the material is homogeneous (this approximation is considered valid, because the glassy sample size was small). At the steady state, there are no internal thermal flows in the material, just the heat produced by the Joule effect, due to the current passing through the material, which is balanced with heat evacuation due to the temperature difference with the ambient

$$V_s I = \frac{V_s^2}{R(T_s)} = K_{th}(T_s - T_a)^n \tag{23}$$

where V_s is the steady-state voltage drop, $R(T_s)$ is the electrical resistance at the equilibrium temperature, T_s, K_{th} is the thermal conductance, and n is a parameter that can range from 1, in Newton's law for cooling, to 1.25, in the phenomenological law that considers that heat exchange with the ambient surrounding the sample, takes place by a natural convection mechanism [23, 24].

Deriving Equations 22 and 23 with respect to I, and substituting values for the turnover point (where $V = V_m$, $T = T_m$ and $dV/dI = 0$), we obtain

$$T_m = \frac{\Delta E}{2nk_B}\left[1 \pm \left(1 - \frac{4nT_a k_B}{\Delta E}\right)^{1/2}\right] \tag{24}$$

where the plus sign corresponds to the point where the second positive differential resistance starts, and the minus sign signifies the point where the CCNDR region appears. An approximate expression for T_m can now be obtained by a McLaurin's expansion of the square root in Equation 24, up to the second term (the error will be, for this type of glassy material, less than 1%)

$$T_m = T_a + \frac{nT_a^2 k_B}{\Delta E} \tag{25}$$

Making $(T_m - T_a)/T_m T_a \approx (T_m - T_a)/T_a^2$, from Equations 22–24, the approximate expression for the turnover voltage as a function of temperature, electrical properties of the glassy material, and the heat evacuation mechanism, is

$$\left(\frac{V_m}{T_a^n}\right)^2 = \frac{nk_B}{e\Delta E} K_{th} R_0 \exp\left(\frac{\Delta E}{k_B T_a}\right) \tag{26}$$

where $e = \exp(1)$.

Fig. 4 shows the steady-state current–voltage characteristics for the glassy alloy $Cu_{0.05}As_{0.50}Te_{0.45}$, between 24 and 52 °C. Lines fitted to the experimental points, have been obtained by a computer simulation program, considering the thermal balance equation, for a non-equilibrium situation and assuming a homogeneous heating of the sample. The expression is as follows

$$C\frac{dT}{dt} = I^2 R(T) - K_{th}(T - T_a) \tag{27}$$

where C is the specific heat per unit volume ($C \approx 1\ J\,g^{-1}\,K^{-1}$ for this type of amorphous material). As in the thermal model on which it is based, the computer simulation program carries out a positive feedback loop. The heat generated by the Joule effect makes the temperature rise, and so the electrical resistance of the sample decreases. This cycle is repeated until the steady state is reached, i.e. when the heat produced by the current and the evacuation due to the temperature difference with the ambient, are balanced (we have considered as valid a minimum temperature increase of 10^{-4} to stop the iterative process). Calculation of the steady-state parameters is repeated at every current value, by means of an algorithm deduced from Equation 27

$$T_{i+1} = T_i + \left[I^2 R_0 \exp\left(\frac{\Delta E}{k_B T_i}\right) - K_{th}(T_i - T_a)^n\right] \times \frac{t_{i+1} - t_i}{C} \tag{28}$$

Parameter n has been deduced by fitting the electrical power generated, at steady state, to the thermal balance Equation 24. Furthermore, the equilibrium temperature has been obtained from the electrical

TABLE I Turnover voltage and thermal conductance, obtained for the sample $Cu_{0.05}As_{0.50}Te_{0.45}$, at different ambient temperatures

T (°C)	V_m (V)	K_{th}, (mW K$^{-5/4}$)
24	28.38	0.54
26	27.17	0.54
28	26.00	0.52
31	24.63	0.46
34	23.18	0.45
37	21.65	0.43
40	20.32	0.43
43	19.09	0.46
46	17.96	0.43
49	17.32	0.45
52	16.92	0.46

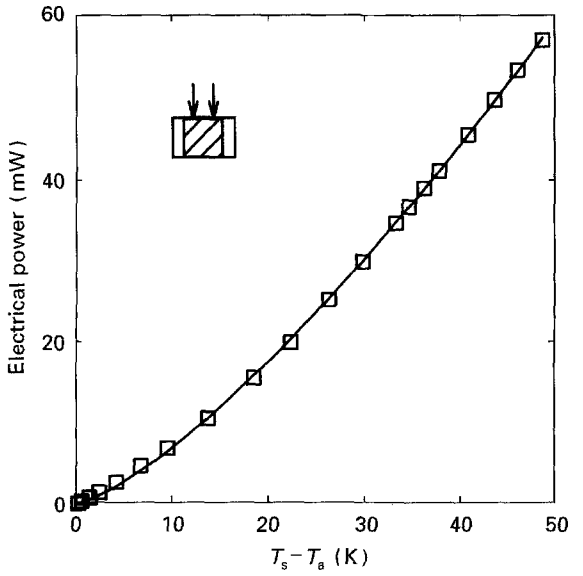

Figure 5 Electrical power generated in a CCNDR experiment versus the difference between the sample and ambient temperatures, at an ambient temperature of 37 °C.

resistance value, by means of the expression

$$T_s = \frac{T_a}{\left[1 + \frac{k_B T_a}{\Delta E} \ln\left(\frac{V_s R_a}{I}\right)\right]} \quad (29)$$

assuming a value for $\Delta E = 0.37$ eV, obtained from the dependence of the electrical resistance on temperature [11].

For every temperature, the experimental values are better fitted to a dependence of natural convection type, i.e. with $n = 1.25$. Table I shows the values of K_{th} obtained; the average value is 0.569 mW K$^{-5/4}$, with a standard deviation of 0.40 mW K$^{-5/4}$ (approximately 8%). Fig. 5 shows the electrical power at steady state versus temperature difference, for an ambient temperature of 37 °C, with the fitted curve following Equation 23, and considering $n = 1.25$.

The experimental results for the turnover voltage, obtained at different ambient temperatures, are also shown in Table I. Although these values are reasonably well fitted to the relationship between the turnover voltage and temperature, deduced from Equation

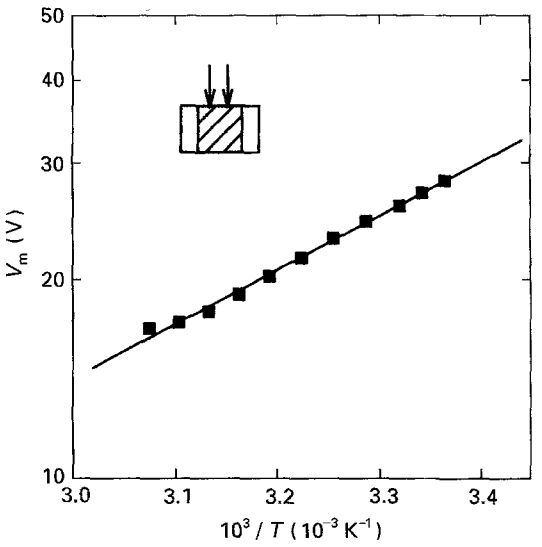

Figure 6 Turnover voltage versus the inverse of ambient temperature.

26, for Newton's law of cooling, i.e. with $n = 1$ [11], better results are obtained when they are fitted to a dependence of the type in Equation 26, considering a natural convection process for the heat exchange between the sample and the ambient. Fig. 6 shows the experimental values for V_m as a function of the inverse of temperature, fitted to Equation 26 by means of a Marquardt–Levenberg type algorithm. In this fitting process, the value of ΔE obtained was 0.38 eV, while the value of R_0 found was 0.0514 Ω, both very close to those obtained in the $\ln R$ versus $1/T$ fitting (0.37 eV and 0.0497 Ω, respectively [11]). This fact certainly confirms the validity of the thermal model used to obtain Equation 26, and also the assumption of a natural convection process for the heat-exchange process.

4.2. Dependence of the turnover voltage on electrode distance

An expression for this dependence can be obtained considering the relationship of the electrical resistance with conductivity, and through this one, with the interelectrode distance

$$R(T) = \frac{d}{A}\left\{1 \Big/ \left[\sigma_0 \exp\left(\frac{-\Delta E}{k_B T}\right)\right]\right\} \quad (30)$$

and comparing this expression with Equation 21, one obtains

$$R_0 = \frac{d}{A\sigma_0} = K_\sigma d \quad (31)$$

where d is the interelectrode distance, A is the cross-sectional area of the sample, σ is the electrical conductivity, and K_σ is a proportionality constant, equal to $(A\sigma_0)^{-1}$. Finally, the expression for the turnover voltage obtained, considering the influence of both temperature and interelectrode distance, is [12]

$$V_m^2 = \frac{K_{th} K_\sigma k_B T_a^{2n} d}{e\Delta E} \exp\left(\frac{\Delta E}{k_B T_a}\right) \quad (32)$$

TABLE II Turnover voltage and electrical resistance obtained at different interelectrodic distances, for the metal–chalcogenide glassy alloy $Cu_{0.05}As_{0.50}Te_{0.45}$

d (mm)	V_m (V)	R (kΩ)
0.85	18.98	16.72
1.02	22.24	20.68
1.30	21.83	27.02
1.49	23.25	30.21
1.85	24.89	35.78
2.35	30.01	41.32

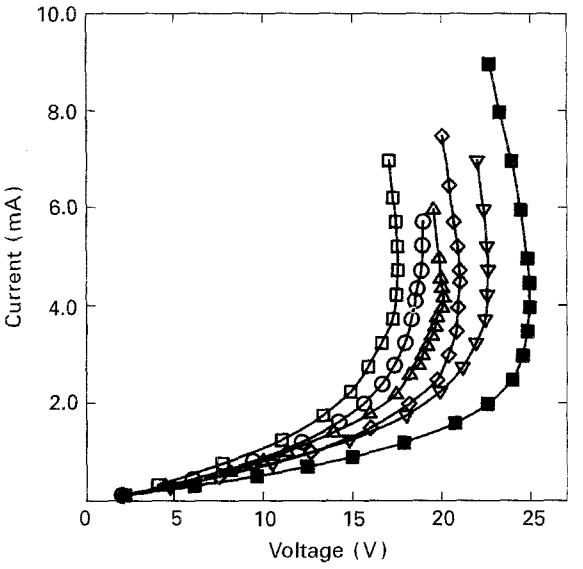

Figure 7 Steady-state current–voltage characteristics for the glassy alloy $Cu_{0.05}As_{0.50}Te_{0.45}$, for different interelectrode distances and at a constant temperature of 30 °C, showing the CCNDR effect. (□) 0.85 mm, (○) 1.02 mm, (△) 1.30 mm, (◇) 1.49 mm, (▽) 1.85 mm, (■) 2.35 mm.

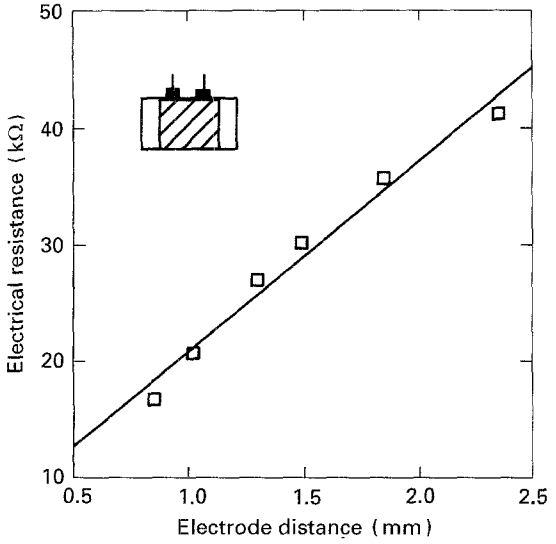

Figure 8 Electrical resistance versus interelectrode distance.

Using the experimental equipment described in Section 2, the steady-state current–voltage characteristics of the semiconductor glassy alloy $Cu_{0.05}As_{0.50}Te_{0.45}$, showing the CCNDR phenomenon, were found for different interelectrode distances. Fig. 7 shows these

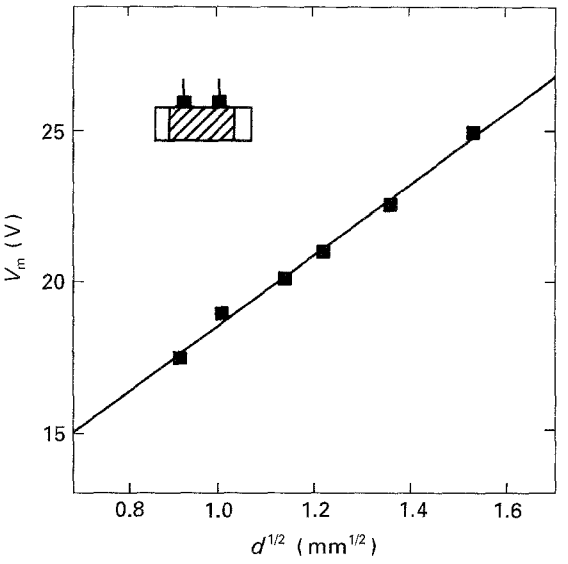

Figure 9 Turnover voltage versus the square root of the interelectrode distance.

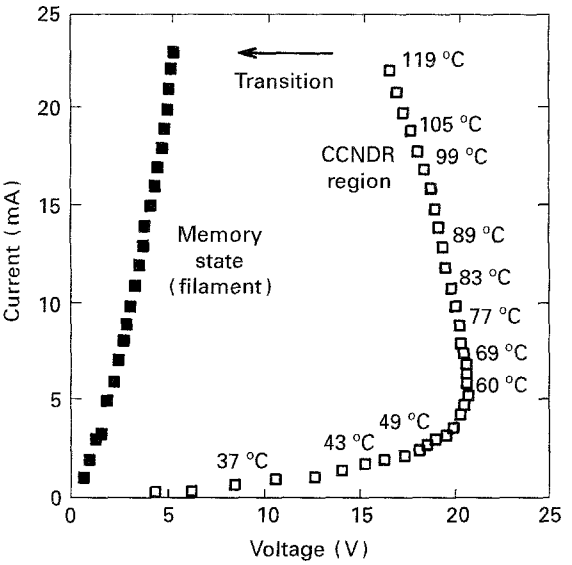

Figure 10 Steady-state current–voltage characteristics at an ambient temperature of 30 °C, showing the CCNDR region, transition to the memory state, and the values of steady-state temperature deduced from Equation 29.

results, which are similar to those found previously for the dependence of CCNDR on temperature. Also, Fig. 8 shows the values of the electrical resistance versus d, in order to confirm the relationship shown by Equation 31. The regression analysis yields a correlation coefficient, r, of 0.996. On the other hand, Fig. 9 shows the experimental values of V_m versus $d^{1/2}$, obtaining a good agreement with Equation 32 ($r = 0.997$), thus confirming the correctness of the assumptions made to obtain these relationships.

Finally, Fig. 10 shows the complete I–V characteristics; the CCNDR region and the transition to the memory (high electrical conductivity) state. So, the I–V characteristics marked as "memory state" in this figure can be considered as those of the crystalline lock-on filament (of quasi-ohmic behaviour). Some

steady-state I–V points have been labelled with the material temperature deduced from Equation 29. Note that the highest value of the material temperature is very close to that of the glass transition temperature for the composition under study (from differential scanning calorimetry measurements, with a heating rate of 5 K min^{-1}, $T_g \approx 130\,^{\circ}C$ [13]).

5. Conclusions

The good agreement of the turnover voltage values, with both the temperature and interelectrode distance relationships found in the present work, is a valid confirmation of the thermal model used to explain the physical process that leads to the CCNDR phenomenon in this type of bulk metal–chalcogenide glassy materials. The basis of this model is the balance between the heat generated by the Joule effect caused by the electrical stimulation, and the heat exchange with the environment, when the steady state has been reached. It has also been shown that the natural convection process represents more precisely the heat exchange between the sample and the ambient which surrounds it. Finally, a computer program has been devised to simulate the behaviour of the sample, once physical parameters (the relationship between the electrical resistance, temperature and thermal conductance) are known.

References

1. S. R. OVSHINSKY, *Phys. Rev. Lett.* **21** (1968) 1450.
2. E. MÁRQUEZ, R. JIMÉNEZ-GARAY, A. ZAKERY, P. J. S. EWEN and A. E. OWEN, *Philos. Mag. B* **63** (1991) 1169.
3. E. MÁRQUEZ, J. B. RAMÍREZ-MALO, J. FERNÁNDEZ-PEÑA, R. JIMÉNEZ-GARAY, P. J. S. EWEN and A. E. OWEN, *Opt. Mater.* **2** (1993) 143.
4. M. I. FRASER, PhD thesis, University of Edinburgh (1982).
5. S. R. OVSHINSKY and H. FRITZSCHE, *IEEE Trans. Electron Dev.* **ED-20** (1973) 91.
6. V. L. VANINOV and S. K. NOVOSELOV, *Inorg. Mater.* **13** (1977) 1573.
7. A. V. DANILOV and R. L. MYULLER, *Zh. Prikl. Khim.* **35** (1962) 2012.
8. D. ADLER, *CRC Crit. Rev. Solid State Sci.* **2** (1971) 317.
9. B. K. RIDLEY, *Proc. Phys. Soc.* **82** (1963) 954.
10. T. M. HAYES and D. D. THORNBURG, in "Proceedings of the 5th International Conference on Amorphous and Liquid Semiconductors" (Taylor and Francis, London, 1974) p. 889.
11. M. DOMÍNGUEZ, E. MÁRQUEZ, P. VILLARES and R. JIMÉNEZ-GARAY, *Semicond. Sci. Technol.* **3** (1988) 1106.
12. *Idem*, in "Proceedings of the 3rd International Workshop on Non-Crystalline Solids (World Scientific, Singapore, 1991) p. 437.
13. E. MÁRQUEZ, J. VÁZQUEZ, N. DE LA ROSA-FOX, P. VILLARES and R. JIMÉNEZ-GARAY, *J. Mater. Sci.* **23** (1988) 1399.
14. E. MÁRQUEZ, L. ESQUIVIAS, P. VILLARES and R. JIMÉNEZ-GARAY, *Rev. Sci. Instrum.* **56** (1985) 1262.
15. E. MÁRQUEZ, P. VILLARES and R. JIMÉNEZ-GARAY, *Phys. Status. Solidi (a)* **102** (1987) 741.
16. *Idem, J. Non-Cryst. Solids* **105** (1988) 123.
17. S. R. DE GROOT, "Termodinámica de los procesos irreversibles" (Alhambra, Madrid, 1968).
18. H. K. ROCKSTAD and M. P. SHAW, *IEEE Trans. Electron. Dev.* **ED-20** (1973) 593.
19. H. FRITZSCHE, *IBM J. Res. Dev.* **13** (1969) 515.
20. E. MÁRQUEZ, M. DOMÍNGUEZ, J. MARTÍNEZ, P. VILLARES and R. JIMÉNEZ-GARAY, *Anal. Fis. B* **86** (1990) 134.
21. R. W. SCARR and R. A. SETTERINGTON, in "Proceedings of IEE", Paper 3176M (1960) p. 395.
22. O. J. M. SMITH, *Rev. Sci. Instrum.* **21** (1950) 344.
23. H. S. CARSLAW and J. C. JAEGER, "Conduction of heat in solids" (Oxford University Press, London, 1959).
24. J. C. JAEGER, *Proc. Camb. Philos. Soc.* **46** (1950) 634.

Received 28 April 1994
and accepted 9 January 1995